Progress in Physics of Applied Materials 5 (2025), Serial Number 9, 119 – 125

Semnan University

Progress in Physics of Applied Materials

journal homepage: https://ppam.semnan.ac.ir/

Round-Shaped Micro Bio-Lasers Utilizing Rhodamine B as a Gain Medium

Shima Vahidi [a], Maryam Aliannezhadi [a*], Zahra Gholizadeh [a]

[a] *Faculty of Physics, Semnan University, P.O. Box: 35195-363, Semnan, Iran*

ARTICLE INFO

Article history:
Received: 6 December 2024
Revised: 20 February 2025
Accepted: 11 March 2025
Published online: 3 May 2025

Keywords:
Bio Laser;
Fluorescence Emission;
Protein;
Microcavity;
Stimulated Emission.

ABSTRACT

Biolasers, new ones that utilize incorporated protein fluorophores within microscale optical cavities to produce coherent light, have a wide range of applications in medicine, including identification, diagnosing, and treating many diseases, skin repair, controlling chemical reactions, pattern generation, etc. Therefore, a new approach to form active microcavities for micro biolaser is proposed based on dye rhodamine B (RhB) and bovine serum albumin (BSA) in the paper. The results indicate the successful production of curved-shaped active cavities. The formed biocavities' average diameters and diameter dispersion are 35.221±0.674 μm and 1.9%, respectively. The output emissions of the device are studied under optical pumping by a Diode-Pumped Solid State (DPSS) laser with the Nd: YAG gain medium operated at 532 nm and an incidence angle of 45º. The output emissions are recorded at different angles, and the high output power is observed at an angle of 90° with the pump angle. Furthermore, the design device has different modes, and the lowest linewidth at half maximum (0.35 nm) and the highest quality factor (2313) are observed at an output wavelength of 809.6 nm. Therefore, the produced laser-activated microcavities can be exploited as suitable options in medical and non-medical optical applications.

1. Introduction

Lasers are widely accepted as indispensable instruments in contemporary polytechnique technology, vanguard scientific research, and matrix medicine. As lasers are used in almost every field such as material analysis and identification, diagnosing and treating many diseases, skin repair, controlling chemical reactions, pattern generation, etc., more attention has been paid to this new technology [1]. Biolasers are a relatively new type of laser; their definition and technology have gradually changed during the past few years due to their wide range of applications. These lasers are now known as a new class of lasers, which employ biological media as part of the laser's active medium or resonant cavity. Furthermore, the lasers residing in biological materials also fall under this category [2]. Biolasers can offer stimulated emission instead of spontaneous fluorescence emission [3]. Biolaser output is superior to conventional fluorescence-based sources due to its strong light intensity (leading to high signal-to-noise ratio), output directional ability (and therefore easy detection and high signal-to-noise ratio), photo feedback mechanism (leading to high sensitivity to small changes in biological processes), threshold behavior (leading to strong image tracking and high contrast ratio in imaging), and narrow linewidth (leading to multi-spectral detection or imaging) [3]. Therefore, different research groups have focused their research on producing bio-lasers using various biological materials.

The first biolasers detected and imaged biological sources such as cells and intracellular changes by placing them inside the active laser medium. Today, materials such as DNA, pectin, cellulose, bovine serum albumin (BSA), duck egg white protein, chicken protein, starch, and various pigments from the albumin family, including indocyanine green, are used to construct these bio-lasers [4-11]. Various cavities, including Fabry-Pérot cavities, microbubble

* Corresponding author. Tel.: +98-912-7317207
E-mail address: ***m_aliannezhadi@semnan.ac.ir***

Cite this article as:
Vahidi Sh., Aliannezhadi M., and Gholizadeh Z., 2025. Round-Shaped Micro Bio-Lasers Utilizing Rhodamine B as a Gain Medium. *Progress in Physics of Applied Materials*, *5*(2), pp.119-125. DOI: **10.22075/PPAM.2025.36146.1124**

cavities, distributed feedback (DFB) cavities, distributed Bragg reflectors (DBRs), photonic crystals, and random cavities, were exploited to provide bio-lasers [12-15]. Spherical microbubbles are often more suitable for creating biolasers due to their interesting properties, including their low threshold, narrow linewidth, and high-quality factor. They were initially suggested in the early 1970s and have been recently widely studied for biomedical and biological applications due to their possible capacities. For the first time, the idea of embedding a laser gain medium using bio-cells was experimentally reported by Gather and Yun in 2011 [16]. The proposed laser contained green fluorescent protein (GFP) sandwiched between two parallel dielectric mirrors.

Since cells have wildly different structures, using different cells leads to lasers with different properties. Early biolasers used biological sources like stationary cells, detecting and imaging intracellular changes by placing them in a laser area [3]. Furthermore, biolasers were made using a variety of materials, including DNA, pectin, cellulose, bovine serum albumin (BSA), duck egg white protein, chicken protein, starch, and various pigments from the albumin family, indocyanine green, and more [4-6, 9]. For example, a solution of chicken albumin and rhodamine B dye was added via micropipette to a polydimethylsiloxane substrate. Then, the heat was applied to remove water from the microspheres and form the laser microcavity [5]. After that, their free spectral range (FSR), and quality factor were then examined. The results showed that the free spectral range was inversely related to the microsphere diameter and decreased with the increasing microsphere diameter. In other studies, a duck egg white with Rh B dye was exploited to produce bio laser [4]. Also, a solution of bovine serum albumin with rhodamine B dye was employed to make round cavities for biolasers [9]. Furthermore, the effects of bovine serum albumin (BSA) concentration were studied, and they found that the cavity diameter and quality factor depend on BSA concentration [17]. In another experiment study, the solution containing starch and rhodamine B dye was established to form the microspheres, and high-quality factor bio cavities were obtained [6]. The subsequent research used alternative biolasers containing dyes, quantum dots, quantum wells, nanowires, fluorescent proteins, and other naturally fluorescent biomaterials to produce the laser's active medium or cavity [18-23].

As mentioned, micro and nano biolasers production is vital due to their properties and extensive applications. Constructing micro biolasers can increase their effectiveness in the body tissues and cell levels. Therefore, this paper focuses on producing the active micro bio cavity to satisfy the requirement. Rhodamine B (RhB) dye exhibits a strong absorption band at 532 nm, leading to simple pumping by available laser sources at about 532 nm. So, the RhB is selected as the gain medium in the study, and bovine serum albumin with some special conditions is used to form round-shaped active microcavities. The novelty of the research is in the method used to provide active cavity of lasers. Different research groups reported the production of micro biocavity by different methods and materials reported in the literature review. However, their method required a higher volume, higher material mass, or more advanced equipment. The method reported in the current work requires no advanced equipment with easy and fast access to active micro biocavity. Furthermore, it is cost-effective and economical.

2. Materials and Methods

The reagents used in this study were; bovine serum albumin (BSA), rhodamine B (RhB), and decanol purchased from Merck company. The bio-cavities were created on a glass slide as the substrate material. To form the bio-cavities, 0.4 g of BSA was dissolved cautiously with 0.5 mL of deionized water at room temperature, reaching homogeneity. In parallel, 0.5 mL of a 1% (w/v) RhB solution was prepared and then added to the BSA solution. An aliquot of decanol was then placed on the glass slide, and 0.5 ml of the mixture was placed on it and allowed to spread out into smaller droplets. This is possible due to the hydrophobicity of the decanol, leading to the rounded and preserved spherical shape of the droplets. Finally, the slide was heated in an oven at 100°C for 50 minutes to evaporate the water and decanol, forming solid microspheres on the substrate. The produced active micro bio cavities were kept in the air at room temperature for further investigations.

3. Results and Discussion

To study the shape and size of cavities, a SaaIran BM-500t optical microscope was used, and the results are displayed in Figure 1 in two magnifications. The results indicate a circular cross-section of the cavities and the formation of three-dimensional cavities due to the appearance of a black shadow around active bio-cavities. Also, it can be concluded that round-shaped active microcavities are produced.

To determine the diameter of the formed round-shaped microcavity, the Digimizer software can be used to record the diameter of active cavities on the substrate, followed by fitting the log-normal function (Equation 1) and calculating average diameter and data dispersion by Equations 2 and 3 [24-26].

$$y(x) = y_0 + \frac{A}{\sqrt{2\pi}}\left(\frac{ln\left(\frac{x}{x_0}\right)^2}{2w^2}\right) \quad (1)$$

$$D = x_0 e^{\frac{w^2}{2}} \quad (2)$$

$$\sigma_D = D\left(e^{w^2} - 1\right)^{\frac{1}{2}} \quad (3)$$

where x and $y(x)$ are the diameters of the formed microcavities on the substrate and their frequency counts in the sample. Furthermore, y_o, x_0, A, and w are fitting parameters of the log-normal function, and D and σ_D are the obtained average diameter of microcavities and their data dispersion, respectively. The histogram diagram of active microcavities and the fitted log-normal function (solid blue line) are presented in the inset of Figure 1, indicating the

diameters of bio cavities are between 5 and 88.222 μm. Furthermore, the average diameter and data dispersion percentage of bio microcavities are 35.221±0.674 μm and 1.9%, respectively.

The different microcavity diameters were also reported in the scientific literature, along with other methods and precursors. The biocavities produced by a drying method have cavity sizes ranging from 10 to 150 μm [1]. Another successful production of bio microcavity was reported using starch instead of bovine serum albumin, and the cavity ranged from 40 to 180 μm [2].

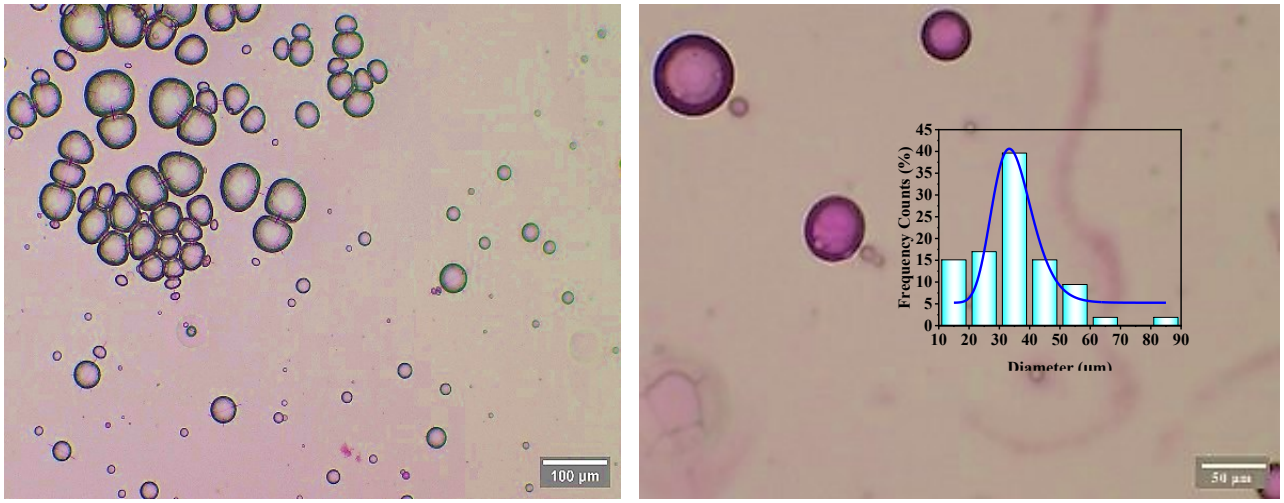

Fig. 1. Optical microscope images of active round-shaped microcavity created using bovine serum albumin and rhodamine B in two magnifications. The histogram diagram of bio microcavities and the fitted log-normal function (solid blue line) are presented in the inset of the image.

Productions of bio microcavity with size distributions of 10 to 120 μm [3] and 20 and 100 μm [4] were also reported. It can conclude that the size range of the formed bio microcavity is 10 to 140 μm, meaning our cavity range is in the reported range of self-forming bio microcavity.

The obtained three-dimensional image with a laser surface profilometer is shown in Figure 2. It can present the surface topography of the formed bioactive laser microcavities by needle on the glass. The results demonstrate the formation of 3D curved-shaped microcavities with a circular cross-section. It is consistent with the optical microscope images of microcavities in Figure 1. Furthermore, the highest height of each formed microcavity by the applied method is in its center. Also, a 2D image of the microcavities on the glass is reported in Figure 3(a). The height versus diameter of the selected microcavity in the yellow marked square in Figure 3(a) was determined using the Gwyddion software and reported in Figure 3(b) to calculate the height of the formed microcavity and estimate the shape of the formed cavities. The computed diameter and height of the microcavities are also depicted in Figure 3(b). The height-to-radius ratio of the formed microcavity is 2h/D=0.34, indicating that the structure has a height less than a hemisphere and is relatively flattened on the surface, which can be related to the hydrophobicity of the surface and the adhesion of the materials during the formation of the microsphere.

As mentioned, the active microcavities contain RhB as the gain medium. Therefore, the absorption and emission spectra of the rhodamine B solution were recorded, and the results are presented in Figures 4(a) and 4(b), respectively, to determine the suitable wavelengths for pumping the microcavities and to identify the available gain region by these active cavities. These optical properties have critical roles in the performance of active microcavities, including determining the suitability of the chosen active medium for special applications and selecting the optical source for pumping these fabricated micro biocavities.

The absorption of the RhB solution was recorded by a Shimadzu UV-165 PC double-beam spectrophotometer, and the results are presented in Figure 4(a). The spectrum has several absorption peaks in different spectral regions (ultraviolet, visible, and infrared); however, the highest absorption is related to the visible region and a wavelength of 524 nm. Also, rhodamine B can absorb wavelengths in the range of 430 to 560 nm in the visible region. Therefore, a green Diode-Pumped Solid State (DPSS) laser with the Nd: YAG gain medium operating at 532 nm can be suitable for pumping the formed active microcavity.

The photoluminescence (PL) spectra of the RhB solution under two excitation wavelengths (320 and 532 nm) were recorded by Shimadzu Spectrofluorophotometer RF-6000, and the spectra were depicted in Figure 4(b). The results show that the output wavelength in the range of 580 nm to 900 nm can be achieved using the design of the active cavity based on rhodamine B. The maximum PL emission of rhodamine B is observed at a wavelength of 625 nm, which can be considered more in laser design.

To study the directionality of the output emission, the schematic diagram depicted in Figure 5(a) was used. The laser incident angle was set θ_i=45°, and the output emission of the active cavity was recorded using a spectrometer at different angles of θ=0°, 45°, and 90°. The laser used to pump the active bio microcavity with the output spectrum shown in Figure 5(b) indicates a Gaussian output with a wavelength of 532.5±0.006 nm and a full width at half maximum (FWHM) of 2.08±0.002 nm. The fitting parameters of the Gaussian function, which fits well to the laser output spectrum, are presented in the inset of Figure 6.

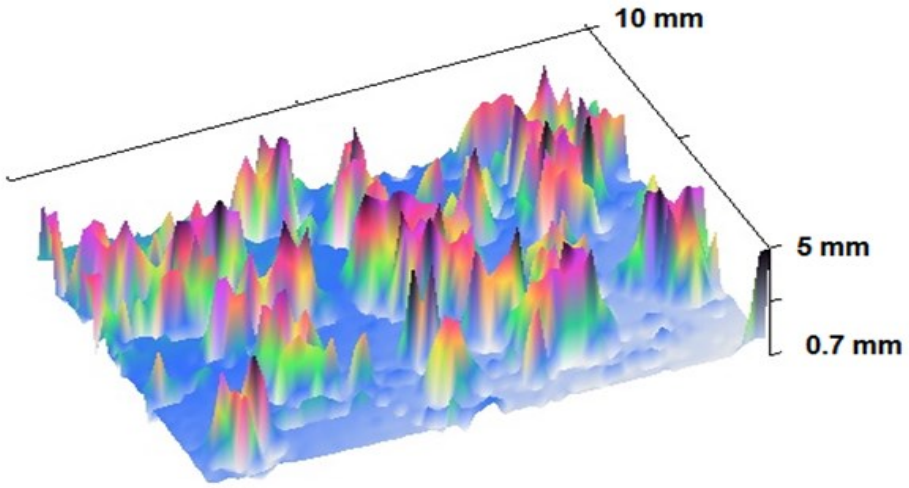

Fig. 2. A surface topography of the formed bioactive laser microcavities by needle on the glass recorded by a laser surface profilometer.

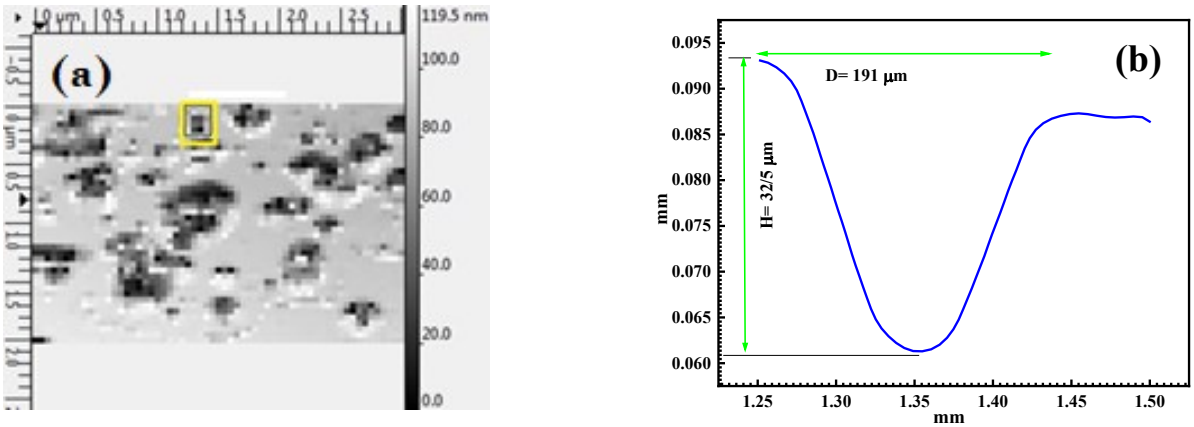

Fig. 3. (a) The surface distribution of height (2D plot) and (b) the height versus diameter of the microcavities created using the needle method on the glass.

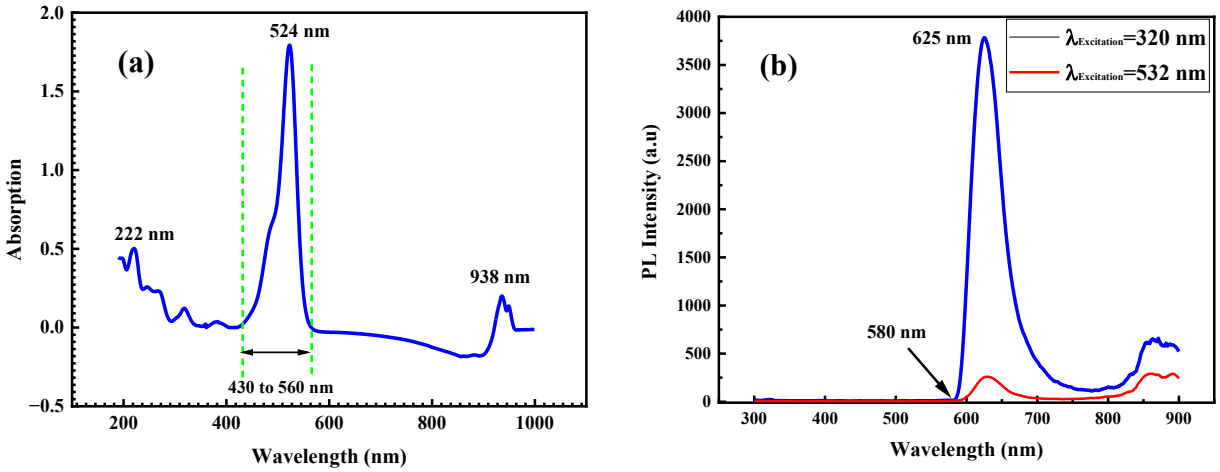

Fig. 4. (a) Absorption spectrum of Rhodamine B solution and (b) Photoluminescence (PL) spectrum of Rhodamine B solution under different excitation wavelengths (320 and 532 nm)

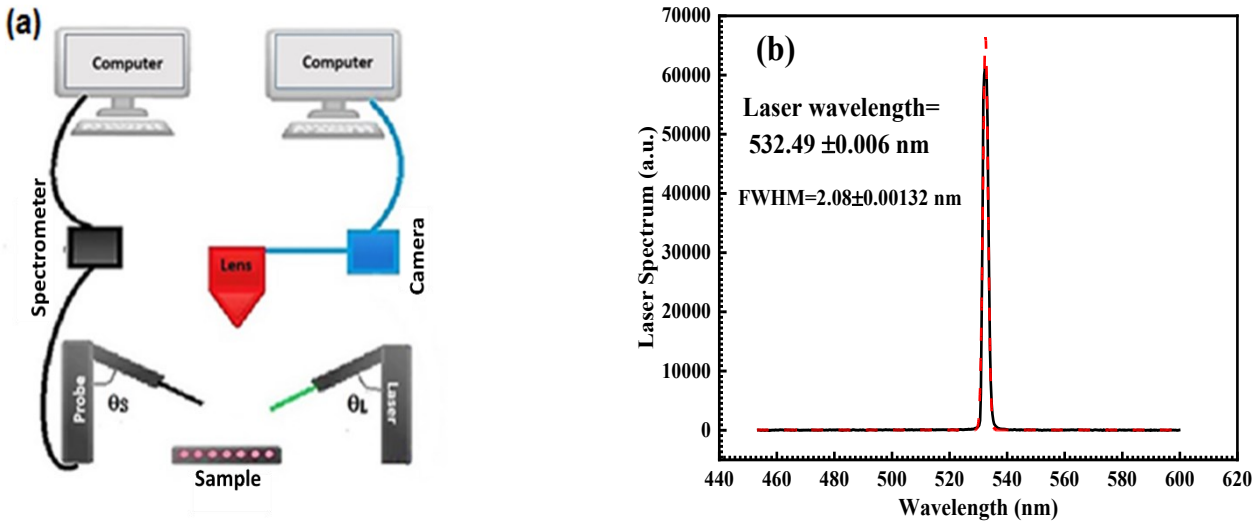

Fig. 5. (a) Schematic diagram of the setup used to excite the microcavity and record output emission, and (b) laser spectrum used to pump the bioactive cavity.

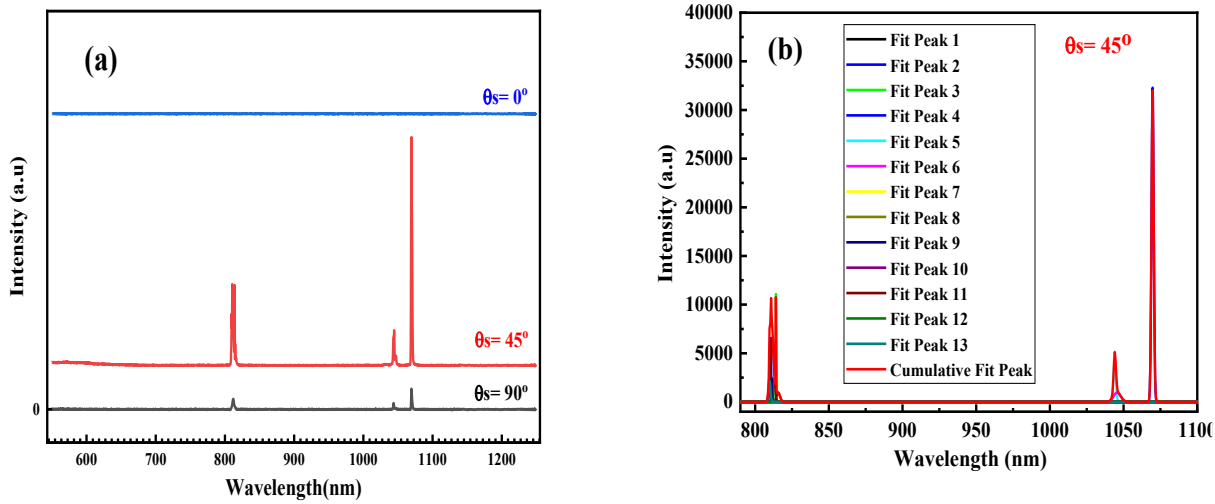

Fig. 6. (a) Output spectra of active microcavity produced with a needle and pumped at 45° with a 532 nm laser at different recorded angles of 0, 45, and 90 degrees, and (b) deconvoluted spectrum at 45° to its Gaussian constructive functions.

Table 1. Output emission of the active bio microcavity excited at 532 nm at an incident angle of 45° and recorded at θ=45°

Recorded angle (Degree)	Central wavelength (nm)	FWHM (nm)	Q Factor
45	809.65	0.35	2313.29
	810.61	0.59	1373.92
	1044.0	1.9	560.5
	1045.6	5.8	179.3
	1069.7	1.8	604.7

The emission spectra dependence of the microcavities to the recording angle was studied by collecting light at angles of θ=0, 45, and 90°, and the results are depicted in Figure 6(a). It can be concluded that the output emission of these active microcavities is directional. No emission can be detected at θ=0°, while the output spectrum of the cavity shows four sharp peaks at ~810, ~811, ~1044, and ~1070 nm at θ=45° with the highest intensity at 1067.9 nm. The recorded intensity at θ=90° is significantly lower than that at 45° and can be ignored. For example, the recorded intensity at 1070 nm at 45 is more than 11 times higher than 90°.

To find more information about the central wavelength, FWHM, and Q factor of every observed mode at the recorded angle of 45°, the spectrum was deconvoluted to its constructor functions by fitting the Gaussian functions to the spectrum, and the results are presented in Table 1. It can be observed that the Q factor of the cavity is high at 1043.9 and 1069.7 nm. Furthermore, Q factors of the microcavity at 809.6 and 810.6 nm are respectively

2313.29 and 1373.92, which are ultra-high-quality factors for the mentioned microcavity, while no specific optical feedback is used to achieve this Q factor, and this feedback is provided only by changing the refractive index of the two boundaries and the curvature of the cavity. A Q factor of 1650 was previously reported for a bio microsphere with a diameter of 49 μm [6]. Furthermore, Q factors of 1790 and 2230 were obtained for the hemisphere and sphere biolasers containing RhB [9]. As one can observe, the current result is comparable with the previously reported studies with different methods. Therefore, it is an interesting and admirable result in producing bio microcavity and micro biolasers. Size dependence free spectral range (FSR) was reported in the scientific literature. A typical FSR of a biolaser containing a bio microsphere with a diameter of 55 nm filled by RhB was 1 nm [5]. The result is consistent with our current study (0.96 nm).

4. Conclusions

Biolasers possess a unique ability to confine light. They facilitate advancements in healthcare, technology, and understanding of biological systems. They have numerous applications in medicine, diagnostics, environmental science, and crucial research. Therefore, in the paper, the successful creation of three-dimensional and curved biolaser active cavities was reported. The dimensions of the produced microspheres and the available operation area of the active microcavity for biolaser production were investigated by studying the optical response of the microspheres under optical excitation at 532 nm. The results demonstrated the directionality of the active bio microcavity and high Q factor of the cavity produced by a fast method.

Funding Statement

This research did not receive any specific grant from funding agencies.

Conflicts of interest

The authors declare that they have no known competing financial interests or personal relationships that could have appeared to influence the work reported in this paper.

Authors contribution statement

Sh.V., M.A., and Z.G. did Conceptualization and methodology and applied software; M.A., and Z.G. investigated validation; Sh.V. did the formal analysis; Sh.V., M.A., and Z.G. did the investigation; Sh.V., M.A., and Z.G. did data curation; Sh.V. wrote the initial draft of the manuscript; M.A., and Z.G. did the review and editing; M.A is the supervisions of the project and the project administration. All authors have read and agreed to the published version of the manuscript. Also, all authors reviewed the manuscript.

Availability of Data and Materials

All data included in this paper are available upon request by contacting the corresponding author.

References

[1] Sun, Y. and Fan, X., 2012. Distinguishing DNA by analog-to-digital-like conversion by using optofluidic lasers.

[2] Fan, X. and Yun, S.H., 2014. The potential of optofluidic biolasers. *Nature methods*, *11*(2), pp.141-147.

[3] Wu, X., Chen, Q., Sun, Y. and Fan, X., 2013. Bio-inspired optofluidic lasers with luciferin. *Applied Physics Letters*, *102*(20).

[4] Van Nguyen, T., Mai, H.H., Van Nguyen, T., Duong, D.C. and Ta, V.D., 2020. Egg white based biological microlasers. *Journal of Physics D: Applied Physics*, *53*(44), p.445104.

[5] Mai, H.H., Nguyen, T.T., Giang, K.M., Do, X.T., Nguyen, T.T., Hoang, H.C. and Ta, V.D., 2020. Chicken albumen-based whispering gallery mode microlasers. *Soft Matter*, *16*(39), pp.9069-9073.

[6] Nguyen, V.T., Nguyen, X.T., Phan, N.N., Le, H.H. and Ta, V.D., 2023. STARCH BASED MICROSPHERE BIOLASERS. *Journal of Science and Technique-Section on Physics and Chemical Engineering*, *1*(01).

[7] Ma, R., Pan, H., Shen, T., Li, P., Chen, Y., Li, Z., Di, X. and Wang, S., 2017. Interaction of flavonoids from Woodwardia unigemmata with bovine serum albumin (BSA): Application of spectroscopic techniques and molecular modeling methods. *Molecules*, *22*(8), p.1317.

[8] Nguyen, T.T., Mai, H.H., Van Pham, T., Nguyen, T.X. and Ta, V.D., 2021. High quality factor, protein-based microlasers from self-assembled microcracks. *Journal of Physics D: Applied Physics*, *54*(25), p.255108.

[9] Van Nguyen, T., 2020. High-quality factor, biological microsphere and microhemisphere lasers fabricated by a single solution process. *Optics Communications*, *465*, p.125647.

[10] Nguyen, T.V., Nguyen, T.D., Pham, N.V., Nguyen, T.A. and Ta, D.V., 2021. Monodisperse and size-tunable high-quality factor microsphere biolasers. *Optics Letters*, *46*(10), pp.2517-2520.

[11] Wu, X., Chen, Q., Sun, Y. and Fan, X., 2013. Bio-inspired optofluidic lasers with luciferin. *Applied Physics Letters*, *102*(20).

[12] Aliannezhadi, M., Mozaffari, M.H. and Amirjan, F., 2023. Optofluidic R6G microbubble DBR laser: A miniaturized device for highly sensitive lab-on-a-chip biosensing. *Photonics and Nanostructures-Fundamentals and Applications*, *53*, p.101108.

[13] Liu, Y., Yang, X., Wang, Y. and Gong, Y., 2024. Fiber Optofluidic Microlasers Toward High-performance Biochemical Sensing. *Optical and Electronic Fibers: Emerging Applications and Technological Innovations*, pp.95-117.

[14] de Armas-Rillo, S., Abdul-Jalbar, B., Salas-Hernández, J., Raya-Sánchez, J.M., González-Hernández, T. and Lahoz, F., 2024. Analysis of Random Lasing in Human Blood. *Biosensors*, *14*(9), p.441.

[15] Prasetyanto, E.A., Wasisto, H.S. and Septiadi, D., 2022. Cellular lasers for cell imaging and biosensing. *Acta Biomaterialia*, *143*, pp.39-51.

[16] Gather, M.C. and Yun, S.H., 2011. Single-cell biological lasers. *Nature Photonics*, *5*(7), pp.406-410.

[17] Van Nguyen, T., Van Pham, N., Mai, H.H., Duong, D.C., Le, H.H., Sapienza, R. and Ta, V.D., 2019. Protein-based microsphere biolasers fabricated by dehydration. *Soft Matter*, *15*(47), pp.9721-9726.

[18] Cortes, F.R.U., Falomir, E., Lancis, J. and Mínguez-Vega, G., 2024. Pulsed laser fragmentation synthesis of carbon quantum dots (CQDs) as fluorescent probes in non-enzymatic glucose detection. *Applied Surface Science*, *665*, p.160326.

[19] Zhang, Y., Shi, B., Zhang, B., Lv, H., Zhang, S., Wang, M. and Wang, X., 2024. Coherent random laser in Enteromorpha prolifera. *Journal of Luminescence*, *275*, p.120760.

[20] Pan, T., Lu, D., Xin, H. and Li, B., 2021. Biophotonic probes for bio-detection and imaging. *Light: Science & Applications*, *10*(1), p.124.

[21] Li, J., Li, X., Zheng, T., Chu, J., Shen, C., Sang, Y., Hu, S. and Guo, J., 2021. Random lasing based on abalone shell. *Optics Communications*, *493*, p.126979. [3] Wu, X., Chen, Q., Sun, Y. and Fan, X., 2013. Bio-inspired optofluidic lasers with luciferin. *Applied Physics Letters*, *102*(20).

[22] Pham, N.V., Nguyen, Q.N., Nguyen, T.V., Nguyen, T.A. and Ta, V.D., 2024. High quality factor, monodisperse micron-sized random lasers based on porous PLGA spheres. *Optics Letters*, *49*(21), pp.6165-6168.

[23] Ta, V.D., Nguyen, T.V., Doan, T.A., Duong, D.C., Caixeiro, S., Saxena, D. and Sapienza, R., 2024. Random lasing in micron-sized individual supraparticles. *Optics Letters*, *49*(14), pp.3886-3889.

[24] Gholizadeh, Z., Aliannezhadi, M., Ghominejad, M. and Tehrani, F.S., 2024. Novel boehmite and η-alumina nanostructures synthesized using a green ultrasonic-assisted hydrothermal method by clove extract for water treatment. *Journal of Water Process Engineering*, *65*, p.105786.

[25] Al-Shemri, M.I., Aliannezhadi, M., Ghaleb, R.A. and Al-Awady, M.J., 2024. Au-H2Ti3O7 nanotubes for non-invasive anticancer treatment by simultaneous photothermal and photodynamic therapy. *Scientific Reports*, *14*(1), p.25998.

[26] Aliannezhadi, M., Doost Mohamadi, F., Jamali, M. and Shariatmadar Tehrani, F., 2025. Ultrasound-assisted green synthesized ZnO nanoparticles with different solution pH for water treatment. *Scientific Reports*, *15*(1), p.7203.